Temporal evolution of the excitonic distribution function in $GaAs/Al_{0.33}Ga_{0.67}As$ superlattices

I. Shtrichman,[1,2] Amiram Ron,[1] D. Gershoni,[1] E. Ehrenfreund,[1] K. D. Maranowski,[2] and A. C. Gossard[2]
[1]*Physics Department and Solid State Institute, Technion–Israel Institute of Technology, Haifa 32000, Israel*
[2]*Materials Department, University of California, Santa Barbara, California 93106*
(Received 12 August 2001; published 20 March 2002)

The thermalization of resonantly excited two-dimensional excitons in $GaAs/Al_{0.33}Ga_{0.67}As$ superlattices is studied using time-resolved photoinduced intersubband absorption. Resonantly photogenerated excitons are sharply distributed in momentum space around the wave vector of their parent photons. We measured the time it takes for these excitons to redistribute evenly over the whole superlattice Brillouin zone and found it to be a few tens of picoseconds. This time depends on the initial density of excitons N_X as $N_X^{-0.7}$ and on the superlattice period L_z approximately as L_z^{-8}. We discuss an excitonic momentum space self-diffusion model, which describes the strong dependence on the superlattice period. We conjecture that exciton-exciton scattering is the dominant cause for this diffusion.

DOI: 10.1103/PhysRevB.65.153302 PACS number(s): 78.66.Fd, 78.47.+p, 78.30.Fs

The dynamics of charge carriers and excitons in semiconductor quantum structures has been a subject for extensive research during recent years.[1–5] Following short-pulse optical excitation, the photogenerated electron-hole (e-h) pairs or excitons are initially phase coherent and their center-of-mass motion has a sharp **k**-space distribution centered at the generating photon momentum. The photogenerated carriers and excitons interact among themselves and with the crystal, and gradually lose their common phase, momentum, and energy. They lose their phase coherence on a subpicosecond time scale[6,7] and their distribution evolves into a thermal one within few picoseconds (ps).[2,3] The thermalized population then reaches thermal equilibrium with the lattice via a slower rate interaction with acoustic phonons.[1]

In this work, we apply time-resolved visible-infrared (IR) dual-beam spectroscopy to directly measure the ps evolution of the excitonic distribution function in superlattices (SL's). By resonantly pumping undoped GaAs/AlGaAs SL's we exclusively photogenerate heavy-hole (HH) excitons with their center-of-mass momentum equal to the photon momentum. By means of exciton-exciton (X-X) scattering, the excitons exchange momentum among themselves, until the entire population eventually reaches thermal distribution. We probe the photoinduced absorption (PIA) spectrum due to optical transitions between the SL conduction subbands and measure its temporal evolution. In the process of probing the SL subband PIA spectrum we temporarily promote an electron from the lowest conduction subband ($E1$) into the first excited one ($E2$). Thus, the probe photon energy is equal to the $E2$-$E1$ energy difference in the presence of a heavy hole in its lowest HH1 level.[8] Therefore, due to the $E1$-$E2$ dispersion, by scanning the probe photon energy, we indirectly measure the $E1$-HH1 excitonic population distribution along the k_z direction in momentum space. For resonant excitation into the $E1$-HH1 exciton, the excitonic population is sharply distributed around the photon wave vector, which is very small. Thus, by measuring the evolution of the PIA spectrum we closely follow the thermalization process of the resonantly excited excitonic population. We note that this evolution is particularly slow in resonant excitation due to two reasons. (i) The characteristic time for an X-X scattering event at low densities is $\simeq 1$ ps,[3] while that for electron-exciton (e-X) scattering is few times faster.[4,5] (ii) In a single X-X scattering event, only a small momentum can be exchanged, since the initial photogenerated excitons carry small momenta. In single e-X, h-X, e-e, or h-h scattering, however, this is not the case.

The evolution in momentum space of resonantly photogenerated excitons can only be indirectly inferred from interband probes, such as photoluminescence, due to the intrinsic small momentum that the probing photon carries.[3,9–13] We circumvent this obstacle by using instead an intersubband probe, which induces an optical transition between the first ($E1$, occupied) and second ($E2$, empty) conduction subbands. Therefore, our photon probe is not subjected to the exclusion principle as in the case of interband pump-probe experiments.[12–15] In addition, due to the difference in the two subband dispersions, the energy of the photon provides a sensitive probe to the momentum state of the electron whose optical transition is being induced.[16]

We study three SL samples grown by molecular beam epitaxy on a (100)-oriented GaAs substrate. Each sample consists of 33 periods of undoped $GaAs/Al_{0.33}Ga_{0.67}As$ quantum wells. The thicknesses of the GaAs/AlGaAs layers in the three SL's were measured by high-resolution *X*-ray diffraction: 50/90 Å, 60/62 Å, and 60/45 Å, respectively. These SL's were specifically designed such that their first electronic level has almost no dispersion along the growth direction, while their second electronic level is considerably dispersed. Due to the dispersion of the $E2$ subband, we directly correlate the $E1$-$E2$ intersubband optical transition energy with the electron crystal momentum along the SL growth direction.

Two edges of each sample were polished at 45° to the growth axis, in order to form a waveguide for the mid-IR radiation with an electric field component parallel to the growth direction. The measurements were done with the samples mounted on a cold finger cryostat at $\simeq 10$ K. The

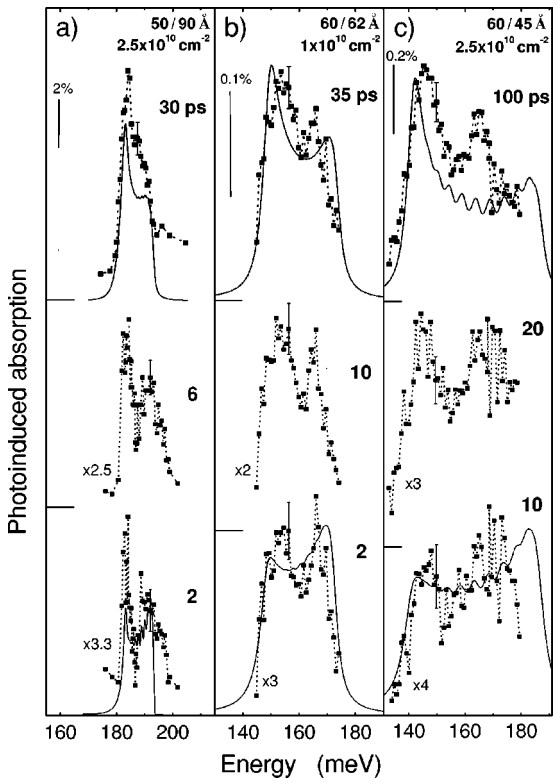

FIG. 1. (a), (b), (c) Photoinduced ISBA spectra at various delay times for the three GaAs/AlGaAs SL samples, respectively, at 10 K and resonant excitation. The overlaid solid lines represent the calculated ISBA with electrons in thermal equilibrium (top) and in non-thermal distribution at the moment of photogeneration (bottom). The spectra are shifted vertically for clarity and the small horizontal lines represent their zero intensity.

details of the time-resolved PIA setup are described elsewhere.[16] The setup allows us to spectrally tune the IR probe pulse and to variably delay it relative to the visible pump pulse. The temporal resolution of the system is $\simeq 4$ ps, and the spectral resolution is 1 meV in both the pump and probe energies. We estimate the exciton density per period from the measured beam average power, repetition rate, and spot diameter on the sample, together with the calculated interband absorption coefficient.

In Fig. 1 we display the photoinduced intersubband absorption (ISBA) spectra under resonant excitation into the lowest heavy-hole excitonic resonance (HH1) for various delay times. Each spectrum is generated by measuring the transient ISBA at various probe energies, and the spectra in Fig. 1 represent constant time cross sections of the measured data. We note that the SL with narrower barriers has a spectrally wider ISBA spectrum. This results from the larger overlap between the $E2$ wave functions in neighboring wells. We find, indeed, that the measured ISBA spectral width agrees quite well with the calculated dispersion of $E2$. The low-energy and high-energy peaks in the spectra are due to the one-dimensional van Hove singularities in the $E1$-$E2$ joint density of states. In all samples we see that at short times the high-energy peak in the spectrum is enhanced relative to the low-energy peak. As time evolves, the high-energy peak loses intensity relative to the low-energy peak, and finally it appears as a low-intensity shoulder on the main, stronger, low-energy peak.

The solid lines (Fig. 1) overlaid on the shortest delay (bottom) and longest delay (top) measured spectra are the calculated ISBA, where we assume a resonant and thermal distribution of the photogenerated excitons, respectively. For these calculations we use an eight-band $\mathbf{k}\cdot\mathbf{p}$ model to calculate the energies, wave functions, and optical transition matrix elements of the charge carriers in the periodic structure.[17] With these quantities at hand, the ISBA spectrum is readily calculated once the number of electrons and their distribution in momentum space are known. In order to find the electronic distribution function, we convolute the excitonic (center of mass) and the relative momentum distribution functions. The initial excitonic distribution function is assumed to be a very sharp function in momentum space centered at the exciting photon momentum, $k_z = k_{ph} = 2\pi n/\lambda$, where n is the refractive index and λ is the photon wavelength in vacuum. The excitonic distribution function eventually evolves into Maxwell-Boltzmann distribution at later times. The e-h relative momentum distribution function is given by the squared Fourier transform of the $1s$ $E1$-HH1 excitonic envelope wave function. Hence, for optical excitation into the HH1 excitonic resonance, the initial electronic $\mathbf{k}^{\mathbf{e}}$-state distribution is given approximately by the relative momentum distribution. In this case, we find that the low-k_z^e states are heavily populated relative to the high-k_z^e states.[16] The result of this nonthermal distribution is a considerable enhancement of the high-energy peak in the calculated ISBA spectrum, as given by the solid lines overlaid on the measured shortest delay time spectra in Fig. 1. After the thermal distribution is reached, the exciton center-of-mass momentum distribution significantly affects the electron momentum distribution. Due to the low dispersion of the excited $E1$ level ($\simeq 1$ meV), the excitons are now almost uniformly distributed along the SL direction, and the resulting ISBA line shape is mainly determined by the $E1$-$E2$ joint density of states. In this case, the low-energy peak in the calculated ISBA final spectrum is increased in intensity relative to the initial spectrum, as shown by the solid lines overlaid the measured spectra at the longest delay time in Fig. 1. We conclude that the time it takes for the initial intersubband spectrum to evolve to its final shape is a quantitative measure of the time it takes for the resonantly photogenerated exciton population to redistribute in momentum space over the whole SL first Brillouin zone (BZ).

In order to extract the redistribution time, we divide the area under the high-energy peak in the spectrum by the area under the whole ISBA spectrum. In Fig. 2 we display this ratio as a function of time, for the three samples. The solid lines represent the best fit of a single-exponential decay function to the data. At this particular exciton density, we find that the redistribution times are 3.3, 7, and 31 ps for the three SL's, respectively. These characteristic times are about an order of magnitude longer than the X-X scattering time at this density ($\simeq 1$ ps).[3] This result is reasonable, since the momentum exchange during the X-X interaction cannot exceed the momentum that a resonantly photogenerated exciton

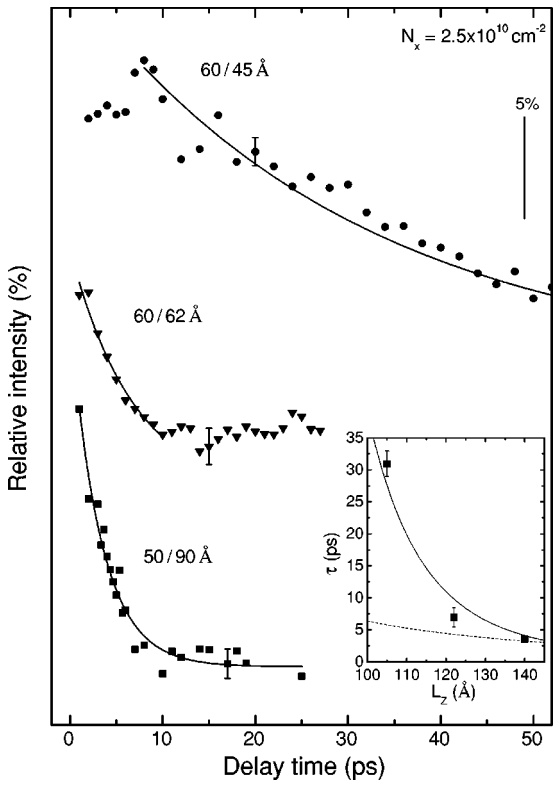

FIG. 2. The intensity of the high-energy peak in the ISBA spectrum relative to the integrated ISBA spectrum (from Fig. 1) vs delay time. The solid lines are single-exponential decay fits that determine the exciton redistribution times (τ). The curves are shifted vertically for clarity. Inset: the redistribution time as a function of the SL period length. The solid (dash) line represents the **k**-space diffusion model using a **k**-dependent (independent) diffusion coefficient.

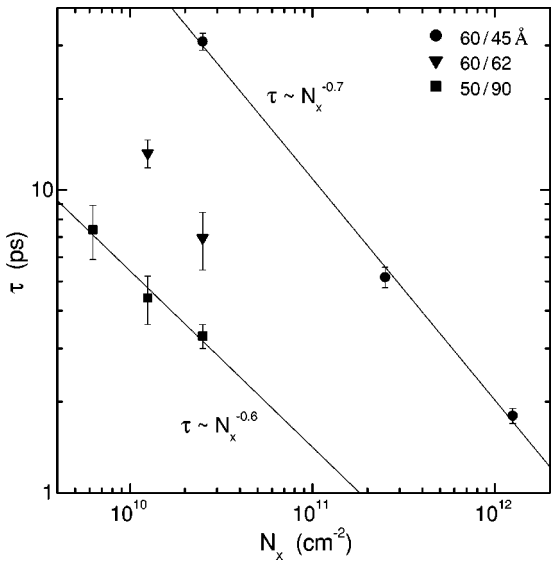

FIG. 3. The redistribution time as a function of the exciton density for the three samples. The solid lines represent the best power law fit to the experimental data.

carries, and therefore, few successive scattering events are needed in order to diffuse the excitons from their initial momentum ($\simeq 0.003$ Å^{-1}) to the edge of the SL BZ ($\simeq 0.02$ Å^{-1}). We note here that for all three SL's, no temporal evolution of the ISBA spectrum was observed once the excitation was tuned to higher energies, off the HH1 resonance. In these cases (not shown here), the temporal evolution of the spectrum is always faster than our temporal resolution due to the much faster scattering processes, which take place when excitons are not the only photogenerated species.[4,5] The characteristic X-X scattering time ($\simeq 1$ ps) is much shorter than the exciton–acoustic-phonon scattering time ($\simeq 100$ ps).[1] For this reason we neglect the interaction with the crystal at low temperatures and conclude that in the case of resonant excitation, the redistribution time ($\simeq 10$ ps) is solely due to X-X interaction. The redistribution of the excitons over the whole SL BZ ends much before complete thermal equilibrium with the crystal is reached. In Fig. 3 we display the momentum redistribution times as a function of the exciton density for the three samples. We find that the redistribution time decreases with increasing exciton density as $\tau \propto N_X^{-0.7}$. Using a classical Fokker-Planck model[18] we find that the X-X interaction rate is expected to be proportional to N_X and to the square of the interaction potential. We suggest that the measured sublinear dependence of the inverse redistribution time on the exciton density is due to the screening of the X-X interaction at high densities.

In the inset to Fig. 2 we display the momentum redistribution time as a function of the SL period for a fixed resonant exciton density of 2.5×10^{10} cm^{-2}. Each data point represents one sample. We find that the redistribution time decreases with increasing SL period as $\tau \propto L_z^{-\alpha}$, with $\alpha = 7.5 \pm 0.6$. This tendency is expected since a longer-period SL has a shorter BZ, and consequently less scattering events are needed in order to complete the redistribution. In order to quantitatively account for this strong dependence, we present a phenomenological model that describes this redistribution as self-diffusion of excitons in momentum space due to scattering among themselves. As indicated above, the temporal evolution of the ISBA spectrum is almost entirely determined by the redistribution of the excitons along the SL BZ. We therefore assume that the time-dependent excitonic momentum distribution function along the SL direction, $f(k_z,t)$, follows a one-dimensional diffusion equation

$$\frac{\partial}{\partial t} f(k_z,t) = \frac{\partial^2}{\partial k_z^2}[D(k_z) f(k_z,t)]. \tag{1}$$

We numerically solve Eq. (1) while imposing periodic boundary conditions on the exciton distribution function at the edges of the SL first BZ: $f(\pi/L_z,t) = f(-\pi/L_z,t)$. The diffusion process in momentum space is temporally simulated by starting, at $t=0$, with a sharp Gaussian distribution function, centered around the exciting photon momentum. As time progresses, $f(k_z,t)$ broadens and eventually becomes almost k_z independent along the whole BZ. In the calculations, we define the redistribution time τ as the time it takes for $f(k_z,t)$ to reach a stage where the relative flatness over the whole BZ is better than 25%, i.e., $\min[f(k_z,\tau)]$

$>\max[f(k_z,\tau)]/4$. For all times $t>\tau$, $f(k_z,t)$ thus obtained yields a reasonable fit to the experimental final spectrum (Fig. 1).

Using this procedure, we calculate the dependence of the redistribution time on the SL period once the diffusion coefficient $D(k_z)$ is known. The dashed line in the inset to Fig. 2 represents a calculation with a k-independent diffusion coefficient. The very weak dependence of the resulting redistribution time on the period length clearly shows that a k-independent diffusion coefficient is not adequate to describe the experimental results. We assume that $D(k_z)$ varies slowly for small k_z but decreases strongly as a power law for $k_z>k_0$, where $2\pi/k_0$ is a characteristic length, which may be related to the wave function coherence length along the superlattice direction. We then write for $D(k_z)$,

$$D(k_z)=\frac{D}{k_z^n+k_0^n}. \tag{2}$$

In Fig. 4 we show the calculated $f(k_z,t)$ for a SL with a period $L_z=150$ Å, using Eqs. (1) and (2). Using the power n and the value of k_0 as fitting parameters, we find that the best fit of this model to the experimental results is obtained for $n=6$ and $k_0\simeq(80\ \text{Å})^{-1}$ (solid line in the inset to Fig. 2). Note that for $n=6$ we would expect from Eqs. (1) and (2) that $\tau\propto L_z^{-8}$. This dependence of the redistribution time on the superlattice period is in accordance with our experimental findings: $\tau\propto L_z^{-7.5\pm0.6}$. The characteristic length $2\pi/k_0\simeq500$ Å found by the fit is $\simeq 3L_z$, which may be interpreted as the exciton coherence length along the SL axis.

We conclude from the above discussion the following. (a) The experimental data strongly point towards the existence of a cutoff (k_0) in k_z. (b) Equation (2) provides a consistent explanation of the period dependence of the redistribution time. Though the power $n=6$ in $D(k_z)$ may point towards the X-X dipole interaction, which couples between the excitons along the SL axis,[19] the exact physical mechanism responsible for the k-space diffusion still requires a more thorough theoretical treatment.

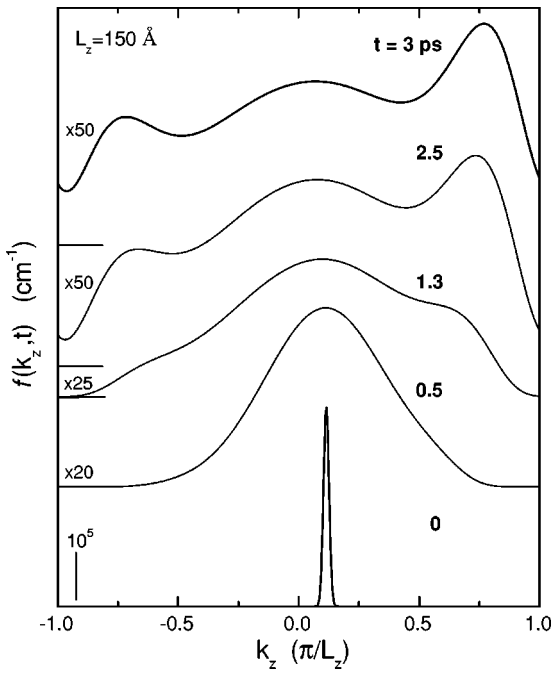

FIG. 4. The calculated excitonic distribution function $f(k_z,t)$ in the SL first BZ for various times after pulsed photogeneration ($t=0$). Here $f(k_z,t)$ is normalized to 2.5×10^{10} excitons per cm^2. The curves are shifted vertically for clarity.

In summary, we used the time-resolved photoinduced intersubband absorption technique to study the temporal evolution of the excitonic momentum distribution following resonant pulsed excitation. We conjecture that the strong decrease of the redistribution time with the SL period length is due to self-diffusion of excitons in phase space.

This research was supported by the Israel Science Foundation founded by The Israel Academy of Sciences and Humanities.

[1] J. Shah, *Ultrafast Spectroscopy of Semiconductors and Semiconductors Nanostructures* (Springer-Verlag, Heidelberg, 1996).
[2] S. Lutgen *et al.*, Phys. Rev. Lett. **77**, 3657 (1996); Solid State Commun. **106**, 425 (1998).
[3] H. Wang, J. Shah, T.C. Damen, and L.N. Pfeiffer, Phys. Rev. Lett. **74**, 3065 (1995).
[4] M. Koch *et al.*, Phys. Rev. B **51**, 13 887 (1995).
[5] A. Honold, L. Schultheis, J. Kuhl, and C.W. Tu, Phys. Rev. B **40**, 6442 (1989).
[6] A. Schülzgen *et al.*, Phys. Rev. Lett. **82**, 2346 (1999).
[7] S. Arlt *et al.*, Phys. Rev. B **62**, 1588 (2000).
[8] The effect of an electron-hole plasma on the intersubband absorption energy is briefly discussed in I. Shtrichman *et al.*, Phys. Rev. B **65**, 035310 (2002).
[9] B. Deveaud *et al.*, Phys. Rev. Lett. **67**, 2355 (1991).
[10] A. Vinattieri *et al.*, Phys. Rev. B **50**, 10 868 (1994).
[11] L.C. Andreani, Phys. Scr. **35**, 111 (1991).
[12] W.H. Knox *et al.*, Phys. Rev. Lett. **54**, 1306 (1985).
[13] P. Vledder *et al.*, Phys. Rev. B **56**, 15 282 (1997); J. Lumin. **83-84**, 309 (1999).
[14] C. Sieh *et al.*, Phys. Rev. Lett. **82**, 3112 (1999).
[15] T. Meier *et al.*, Phys. Rev. B **62**, 4218 (2000).
[16] R. Duer *et al.*, Phys. Rev. Lett. **78**, 3919 (1997); Superlattices Microstruct. **17**, 5 (1995).
[17] D. Gershoni, C.H. Henry, and G.A. Baraff, IEEE J. Quantum Electron. **29**, 2433 (1993).
[18] F. Reif, *Fundamentals of Statistical and Thermal Physics* (McGraw-Hill, Singapore, 1965).
[19] C. Cohen-Tannoudji, B. Diu, and F. Laloë, *Quantum Mechanics* (Wiley, New York, 1997), Vol. II, Chap. C_{XI}.